Vehicle Cruise and Lateral Control

Yuxuan Sheng (SID: 510592563)
Dept. of Aerospace Engineering
The University of Sydney
Sydney, Australia
yshe8026@uni.sydney.edu.au

I. Introduction

The Mercedes AMG GT Black Series (Fig. 1) is a high-performance sports car featuring a 720 hp V8 engine, aerodynamic design, and luxurious interior. Designed for peak performance on both the track and the road, it set a 0-100 kph time of 3.1 seconds and an electronically limited top speed of 325 kph [1]. As a street-legal vehicle, it incorporates meticulously engineered Cruise Control and Lateral Control systems. This paper examines the system dynamics behind these functions and proposes simplified designs for the exact car model. However, Mercedes' actual design is more advanced and certified as road legal in most countries, unlikely derived from linearization of dynamic equations.

For our purposes, we employ linearized equations to represent the plant models for both cruise and lateral control. The controllers dedicated to reference tracking are tuned based on these linear assumptions. We utilize MATLAB Simulink to conduct simulations that validate their functionality. All relevant parameters for this paper are compiled in table I.

Fig. 1. An AMG GT Black Series from the garage, which features custom rear wing. The drag coefficient (C_D) and frontal area (A) of this vehicle may slightly differ from the standard model.

II. Longitudinal Controller

A. Linearization

We can choose to linearize our dynamic equation at three distinct speeds: (1) a typical urban cruise speed of 60 kph, (2) a typical highway cruise speed of 120 kph, and (3) an Autobahn cruise speed of 325 kph.

TABLE I
Mercedes AMG GT Operation Parameters

Relevant Parameters			
Parameter	***Symbol***	***Value***	***Unit***
Air Density	ρ	1.225	kg/m^3
Drag Coeff.	c_D	0.42	–
Frontal Area	A	2.12	m
Lumped Term	$\frac{1}{2}A\rho c_D v^2$	0.545	kg/m
Kerb Weight	m_k	1540	kg
Driver Weight	m_d	50	kg
TOT Weight[a]	m	1590	kg
Wheelbase	$l_f + l_r$	2.63	m
Width	w	2.01	m

[a] $m = m_k + m_d$.

The corresponding equilibrium points can be obtained via the equilibrium condition $\dot{v}|_{v=v_e} = 0$:

$$m\dot{v} + \frac{1}{2}A\rho c_D v^2 = u \tag{1}$$

$$u_e = \frac{1}{2}A\rho c_D v_e^2$$

$$u_e = 0.545 v_e^2 \tag{2}$$

From eq. (2), the three equilibrium points are calculated accordingly: (1) (16.67 m/s, 151.4 N), (2) (33.33 m/s, 605.4 N) and (3) (90.28 m/s, 4442 N).

Following this, linearization can be carried out:

$$\dot{v} = f(v,u) = \frac{1}{1590}u - \frac{0.545}{1590}v^2 \tag{3}$$

$$\approx \frac{\partial f}{\partial v}\Big|_{(v_e,u_e)}(v - v_e) + \frac{\partial f}{\partial u}\Big|_{(v_e,u_e)}(u - u_e) \tag{4}$$

where

$$\frac{\partial f}{\partial v}\Big|_{(v_e,u_e)} = -2 \times \frac{0.545}{1590} v_e$$
$$= -\frac{1.09}{1590} v_e \quad (5)$$
$$\frac{\partial f}{\partial u}\Big|_{(v_e,u_e)} = \frac{1}{1590} \quad (6)$$

Substituting values, eq. (4) becomes:

$$\dot{v} = -\frac{1.09}{1590} v_e (v - v_e) + \frac{1}{1590}(u - u_e) \quad (7)$$

Alternatively, we can write:

$$\delta\dot{v} = -\frac{1.09}{1590} v_e \delta v + \frac{1}{1590}\delta u \quad (8)$$

When the system is linearized at point (1) (60 kph):

$$\dot{v} = -\frac{18.17}{1590}(v - 16.67) + \frac{1}{1590}(u - 151.4) \quad (9)$$
$$\dot{v} = -\frac{18.17}{1590} v + \frac{1}{1590} u + \frac{151.5}{1590} \quad (10)$$

When the system is linearized at point (2) (120 kph):

$$\dot{v} = -\frac{36.33}{1590}(v - 33.33) + \frac{1}{1590}(u - 605.4) \quad (11)$$
$$\dot{v} = -\frac{36.33}{1590} v + \frac{1}{1590} u + \frac{605.5}{1590} \quad (12)$$

When the system is linearized at point (3) (325 kph):

$$\dot{v} = -\frac{98.41}{1590}(v - 90.28) + \frac{1}{1590}(u - 4442) \quad (13)$$
$$\dot{v} = -\frac{98.41}{1590} v + \frac{1}{1590} u + \frac{4442}{1590} \quad (14)$$

where v should be in units of meters and u in units of Newtons.

By supplying the equilibrium points along with their corresponding equilibrium control inputs u_e, eq. (10), eq. (12), and eq. (14) are simulated in MATLAB Simulink to obtain the system response (acceleration curves). The results are presented in Fig. 2 and table II.

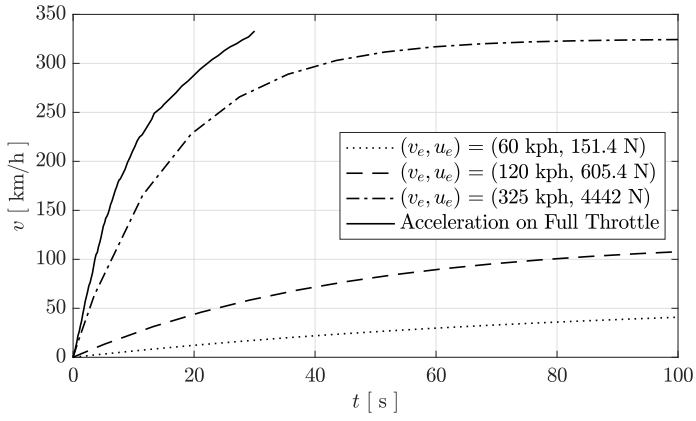

Fig. 2. Variation of vehicle speed over time for three distinct linearization models is shown. The control inputs are set at their respective equilibrium values (u_e), and the initial condition is $v(0) = 0$.

TABLE II
RESPONSE PROPERTIES

Linear Model Response			
Linearized Point (v_e, u_e) ***[m/s, N]***	***Input*** u_e ***[N]***	***Rise Time*** t_r ***[s]***	***Settling Time*** t_s ***[s]***
(16.67, 151.4)	151.4	184.00	387.88
(33.33, 605.4)	605.4	96.00	394.85
(90.28, 4442)	4442	40.00	396.49

In Fig. 2, the three trajectories exhibit similar patterns, increasing and gradually approaching their respective equilibrium values. Notably, as the values of $u = u_e$ increase, the rise time (t_r) decreases. The solid trajectory demonstrates the car's performance at full throttle. Without traction control, the car accelerates to 60 kph in 2 seconds and reaches 120 kph in 5 seconds [3]. Achieving the electronically controlled top speed of 325 kph takes 29 seconds. The actual top speed, without electronic speed control, is 350 kph. The full throttle test represents the ultimate limit that the speed trajectory should never surpass. If the control system demands acceleration beyond the vehicle's physical capabilities, a power deficit would occur, resulting in either a breakdown of the system equation or the acceleration curve following the full throttle acceleration profile.

B. Controller Design

A PID controller is an appropriate choice for cruise control. The proportional, integral, and derivative gains (K_p, K_i, and K_d) can be determined through manual tuning. The reasons for selecting a PID controller are as follows:

- In a PID controller, K_p affects the response strength to errors, with higher values providing faster responses but potentially causing overshoot and instability. K_i eliminates steady-state errors, with higher values increasing error correction speed but potentially causing overshoot and oscillations. K_d anticipates future errors and dampens oscillations, with higher values improving stability and response but potentially amplifying noise. Balancing these gains is crucial for optimal system performance.

- For a step input such as a reference speed, the static state error of a PID controller is zero, because the integral term ensures that the steady-state error is eliminated. (Note, for other types of inputs such as ramps or parabolic inputs, the static state error may not be zero). In the case of a PID controller, the static state error under a constant disturbance (such as a constant gravity component when climbing a slope) can be zero. This is because the integral term in the PID controller accumulates the error over time and adjusts the control signal accordingly, eventually compensating for the constant disturbance and driving the steady-state error to

zero.

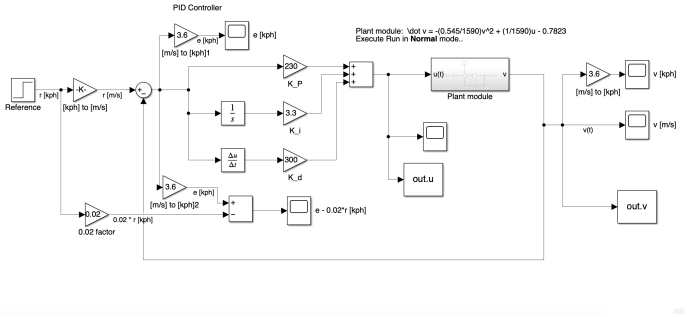

Fig. 3. MATLAB Simulink [4] linearized model with PID controller (K_p = 230, K_i = 3.3, K_d = 300).

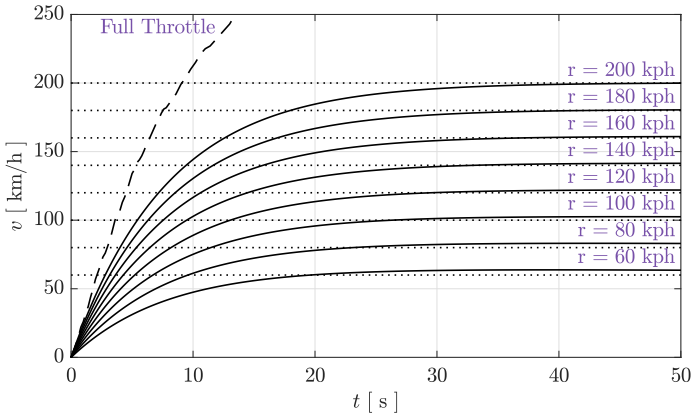

Fig. 4. Acceleration curves for different cruise speed settings using a PID control with K_p = 230, K_i = 3.3, K_d = 300

As depicted in Figure 4, when the linearization is centered around an equilibrium speed (v_e) of 120 kph, a typical highway cruising speed, different speed settings yield equilibrium speeds within 5% of the reference. Given the speedometer offset required by regulators, it is highly improbable for the cruise speed to exceed 5% of the speed limit on public roads. While linear modeling and PID control have their limitations, this control system can maintain speeds ranging from 60 kph to 200 kph with minimal deviation. All system responses fall within the acceleration curve under full throttle conditions (TCS off) [3].

Rise times (t_r) and settling times (t_s) are compiled in table III. These calculations are performed using MATLAB functions. In theory, rise times and settling times can be obtained analytically. However, the theoretical calculations below did not yield similar t_r and t_s values compared to the simulation. For a detailed explanation of the derivation steps, please refer to section V-A.

TABLE III
CONTROLLER TEST

Model Response Under PID Controller K_p = 230, K_i = 3.3, K_d = 300			
Plant Model & Disturbance	***Reference r [kph]***	***Rise Time t_r [s]***	***Settling Time t_s [s]***
Linear Model Centered at v_e = 120 kph & No Disturbance	60	13.09	29.33
	80	13.34	29.32
	100	13.51	29.32
	120	13.62	29.33
	140	13.70	29.32
	160	13.76	29.32
	180	13.81	29.32
	200	13.85	29.32
Nonlinear Model & 8 % grade Incline Type Disturbance	60	41.28	98.79
	80	31.71	98.90
	100	27.19	98.96
	120	24.84	98.99
	140	23.49	99.02
	160	22.66	99.04
	180	22.11	99.06
	200	21.75	99.07

The rationale for the values of K_p, K_i, and K_d used in the Simulink Model (Fig. 4) is primarily empirical. This combination results in an overdamped system that is largely free of overshoots. A K_p value of 230 ensures that the vehicle does not exceed its performance limits. A K_i value of 3.3 eliminates steady-state error without introducing significant overshoot. A K_d value of 300 provides some resilience to input disturbances (which is beneficial in slope-climbing tests) without substantially compromising rise time.

C. Validations

To evaluate the effectiveness of our PID controller, we apply it to the original nonlinear dynamics, incorporating an additional input disturbance in the form of an 8% grade slope.

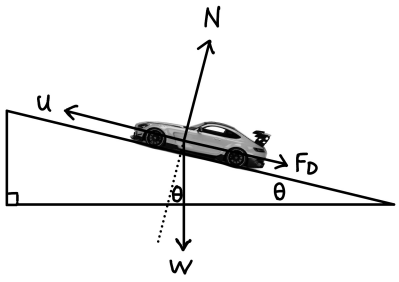

Fig. 5. FBD of AMG GT Black Series on slope.

If the vehicle encounters a steep slope with an 8% grade, the free body diagram can be visualized in Figure 5. The equation of motion is as follows:

$$F = ma \tag{15}$$

$$u - F_D - W\sin\theta = ma \tag{16}$$

$$m\dot{v} + \frac{1}{2}A\rho c_D v^2 = u - mg\sin\theta \tag{17}$$

eq. (17) is of the form

$$m\dot{v} + \frac{1}{2}A\rho c_D v^2 = u - d \tag{18}$$

$$d = mg\sin\theta \tag{19}$$

Without making any changes to the PID controller, the plant model described by eq. (18) is implemented in MATLAB Simulink (Fig.6). Following a similar approach as before, the system response is simulated for a range of reference cruise speeds from 60 kph to 200 kph, and the results are displayed in Fig.7.

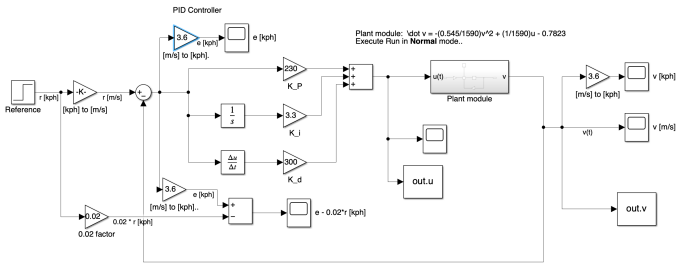

Fig. 6. MATLAB Simulink linearized model applied to original system with disturbance (slope of 8% grade)

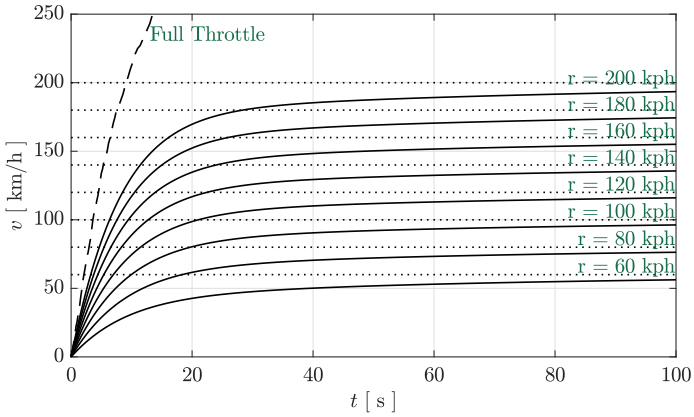

Fig. 7. Demonstration of acceleration curves of linearized model applied to original system with disturbance (slope of 8% grade)

In Fig 7, we observe that the PID controller with the same gain values (derived from the linearized model) still performs reasonably well in achieving the reference speed, even under the disturbance of an 8% grade ramp. However, the settling time is significantly longer. During tuning, we discovered that moderately increasing K_i substantially reduces the steady-state error before overshoot becomes an issue. Increasing K_p improves the rise time, while increasing K_d enhances the settling time when a disturbance is present.

In summary, the controller demonstrates robustness when confronted with a constant disturbance to the input.

III. LATERAL CONTROLLER

A. Linearization

Next, we aim to explore the system dynamics of lateral motion and assess the feasibility of designing a controller capable of automatically executing lane changes under highway cruise conditions.

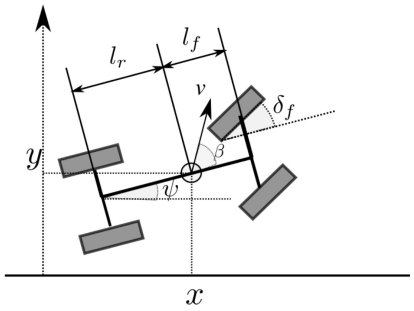

Fig. 8. Illustration of various angles related to steering.

During cruising, the motion of the vehicle's center of mass is governed by:

$$\dot{x} = v\,cos\,(\phi + \beta) \tag{20}$$

$$\dot{y} = v\,sin\,(\phi + \beta) \tag{21}$$

$$\dot{\psi} = \frac{v}{l_r}\,sin\,(\beta) \tag{22}$$

where

$$tan\,(\beta) = \frac{l_r}{l_f + l_r}\,tan\,(\delta_f) \tag{23}$$

In eq. (21) and eq. (22), δ_f represents the steering angle of the front wheels (assuming a zero toe angle), while ψ is the rotation angle of the car with respect to the road direction, as illustrated in Fig 8. The angle β denotes the angle between the center of mass's direction of motion and the car's centerline. With perfect traction, β is smaller than δ_f and is determined by δ_f. In oversteer situations (such as a power slide [5]), β can be larger than δ_f. However, we will not consider understeer or oversteer, as highway cruising remains well within the car's steering performance limits.

From table I, the wheelbase ($l_f + l_r$) of the AMG GT Black Series is 2.630 m. As the center of mass is considered a trade secret and is not publicly available, we assume it is situated in the middle of the wheelbase, resulting in $l_f = l_r$ = 1.315 m.

Assuming constant speed motion $v(t) \approx v_0 > 0$ with small front wheel steering angles ($\leqslant 10^\circ$) [5], (or $\phi \approx 0$, $\beta \approx 0$, $\delta_f \approx 0$), we obtain:

$$tan\,(\beta) = \frac{l_r}{l_f + l_r}\,tan\,(\delta_f)$$

$$\beta = \frac{1}{2}\delta\,f$$

$$\dot{\beta} = \frac{1}{2}\dot{\delta}_f \tag{24}$$

and

$$\begin{aligned}\dot{\psi} &= \frac{v}{l_r}\, sin\, \beta \\ \dot{\psi} &= \frac{v}{l_r}\, \beta \\ \dot{\psi} &= \frac{v}{l_r}\frac{1}{2}\delta_f \\ \dot{\psi} &= \frac{1}{2}\frac{v}{l_r}\delta_f \end{aligned} \tag{25}$$

which leads to

$$\begin{aligned}\dot{y} &= v\, sin\, (\psi + \beta) \\ \dot{y} &= v\, (\psi + \beta) \\ \ddot{y} &= v\, (\frac{1}{2}\frac{v}{l_r}\delta_f + \frac{1}{2}\dot{\delta_f}) \\ \ddot{y} &= \frac{1}{2}\frac{1}{l_r}v^2\delta_f + \frac{1}{2}v\,\dot{\delta_f} \end{aligned} \tag{26}$$

Assuming $y = C_1 e^{st}$ and $\delta_f = C_2 e^{st}$, we can rewrite eq. (26) as:

$$\begin{aligned} s^2 C_1 e^{st} &= \frac{1}{2}\frac{1}{l_r}v^2 C_2 e^{st} + \frac{1}{2}v\, s\, C_2 e^{st} \\ s^2 C_1 &= \frac{1}{2}\frac{1}{l_r}v^2 C_2 + \frac{1}{2}v\, s\, C_2 \qquad (e^{st} \neq 0) \\ G(s) &= \frac{C_1(s)}{C_2(s)} = \frac{A\, s + B}{s^2} \end{aligned} \tag{27}$$

where

$$\begin{aligned} A &= \frac{1}{2}v \\ &= \frac{1}{2}v_0 \end{aligned} \tag{28}$$

$$\begin{aligned} B &= \frac{1}{2 \times 1.315\text{m}}v_0^2 \\ &= \frac{100}{263}v_0^2\ \text{m}^{-1} \end{aligned} \tag{29}$$

In parameters A and B, the constant cruise speed v_0 should be in meters per second.

We have now obtained the second-order differential equation describing the dependence of $y(t)$ on $\delta_f(t)$ (eq. (26)), which gives us the transfer function from the front wheel steering angle δ_f to the lateral position y (eq. (27)).

B. Controller Design

Initially, a PID controller is chosen for controlling the front wheel steering angle, $u = \delta_f$:

$$u = K_p(r - y) + K_i\int_0^t (r - y)d\tau + K_d(\dot{r} - \dot{y}) \tag{30}$$

$$\dot{u} = K_p(\dot{r} - \dot{y}) + K_i(r - y) + K_d(\ddot{r} - \ddot{y}) \tag{31}$$

$$\ddot{y} = \frac{1}{2}\frac{1}{l_r}v^2 u + \frac{1}{2}v\,\dot{u} \tag{32}$$

where eq. (30) is carried out by the Simulink controller model and eq. (31) & eq. (32) is carried out by the plant model (Fig. 10). In hindsight, the car need to respond quickly, the steady state position is of less importance. Therefore a PD controller is sufficient for the task, reducing K_i to zero, as shown in Fig. 9.

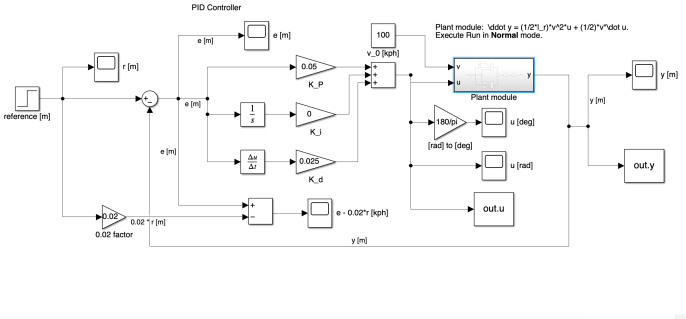

Fig. 9. Lateral motion PD controller model ($K_p = 0.05$, $K_d = 0.025$).

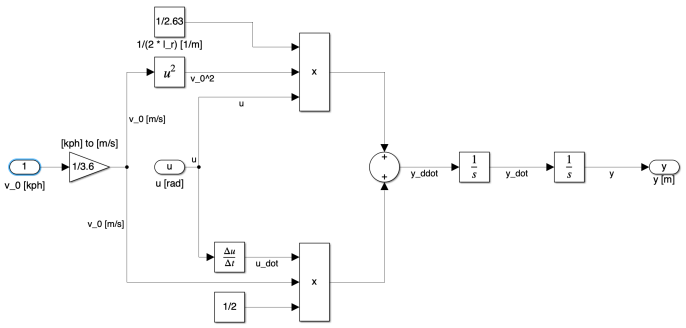

Fig. 10. Lateral motion plant with linear dynamics.

The rationale behind the K_p and K_d values used in the Simulink model (Fig. 9) is also based on empirical evidence. With the combination of $K_p = 0.05$ and $K_d = 0.025$, the lane change execution is optimized for a wide range of highway cruising speeds. The resulting lane change maneuvers are quick and precise, adhering to international driving standards.

C. Validations

The closed-loop system response under the PD controller is tested at a range of cruise speeds from 60 kph to 200 kph on the Autobahn (with a 3.5 m lane width). The lane change is smooth, and the overshoots do not cause the car to drift into an adjacent lane (considering the car width of $w = 2.01$ m). From Fig.11 and Fig.12, we can see that the lane change essentially occurs within 3 seconds and around 80 meters, which is typical behavior exhibited by an average human driver. The lane change is smooth and has minimal overshoot for a wide range of cruising speeds. As the cruise speed increases, the overshoot becomes less pronounced.

One issue with PD or PID controllers is their inability to produce a spatially and temporally symmetric response when

using a constant reference. Additionally, shaping the response with a variable reference can be challenging. A symmetric response, resembling the shape of a Sigmoid function, is more desirable for the following reasons:

- As depicted in Fig. 14, under the assumption of a linear 1:1 steering ratio, the steering wheel motion exhibits neither spatial nor temporal symmetry. The PD controller requires an abrupt 10-degree steering input right after the simulation commences. In reality, this would impose significant stress on the tires and induce understeer. Such a destabilizing input would render the car's behavior more challenging to predict, as driving beyond its performance limit would involve increasingly complex dynamics.

- While the initial input is generally adequate for executing a lane change, cornering requires taking tire behavior into account. To initiate a left turn, it is advised to steer slightly right first. As the car moves a little to the right on a straight path, its tires experience resistance and shear in the same direction as if it were turning left. By replicating this behavior, the control system could distribute the load on the tires more gradually. It is crucial to avoid driving beyond the performance limit, as additional control authority is necessary for evasive maneuvers on highways.

- It is essential for other road users to have sufficient time to interpret our vehicle's intentions. A sudden veering to the left could increase the risk of a collision, particularly when other vehicles are in close proximity. On the Autobahn, speed differences can be substantial, with some vehicles cruising at over 300 kph. Gradually initiating the lane change at the beginning is optimal. While this approach might seem inexperienced, it allows our vehicle the opportunity to abort the lane change if necessary and provides the rapidly approaching vehicle behind a chance to execute evasive maneuvers.

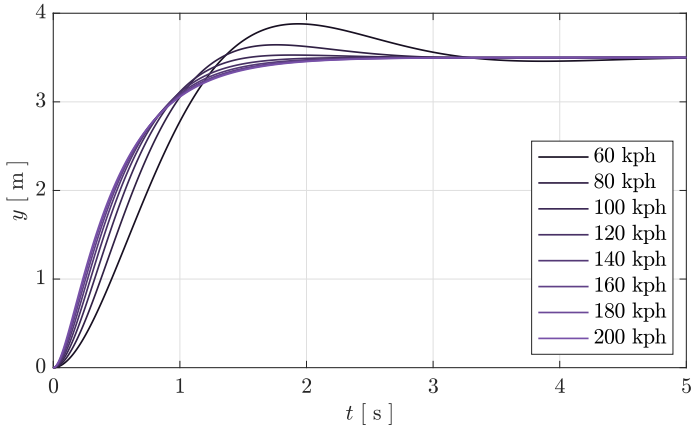

Fig. 11. Lateral response when cruising forward.

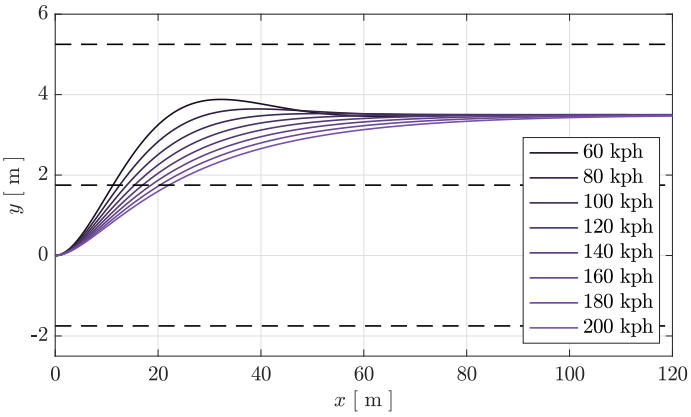

Fig. 12. Lane change trajectory with Autobahn standard dividers (Lane width = 3.5 m).

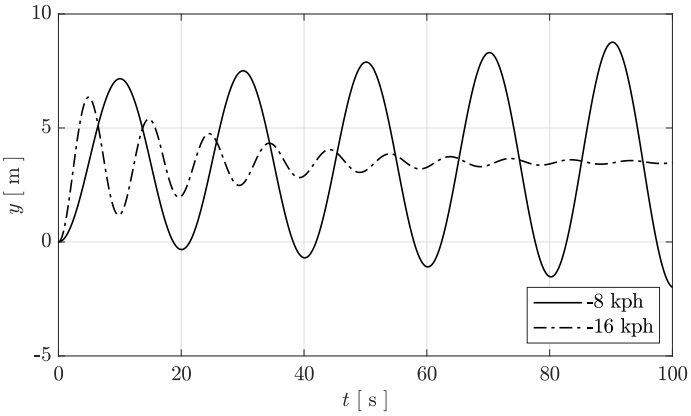

Fig. 13. Lateral response when cruising in reverse.

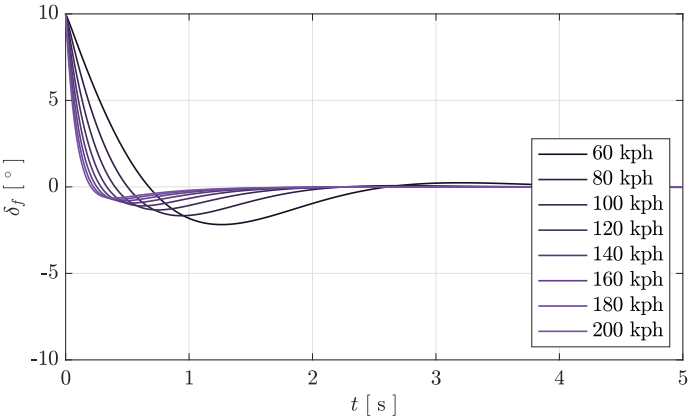

Fig. 14. Front wheel steering angle for the lane change.

When the transfer function (eq. (27)) is zero:

$$As + B = 0 \tag{33}$$

$$s = -\frac{B}{A}$$

$$s = -\frac{\frac{1}{2}\frac{1}{l_r}v^2}{\frac{1}{2}v}$$

$$s = -\frac{1}{l_r}v \tag{34}$$

When $v < 0$, $s > 0$, the system is unstable. For $v = -8$ m/s, $s = 6.08$ s^{-1}, and for $s = 12.17$ s^{-1}. As demonstrated in Fig. 13, our PD controller is unable to stabilize reverse cruising within the 100-second time window. For -8 kph reverse cruising, the response eventually settles down, albeit over an extended period. However, for -16 kph reverse cruising, the oscillatory response amplifies over time. Evidently, for this particular system, instability and poor controller performance arise when the transfer function approaches zero.

A PD or PID controller is designed to control stable or marginally stable systems. It is generally not suitable for controlling statically unstable systems, which are inherently unstable and typically require more advanced control techniques or appropriate feedback mechanisms.

The zero of a transfer function is identified as the value of s that causes the transfer function to approach zero. For the transfer function in eq. (27), the zero occurs at $s = -\frac{1}{l_r}v$. When s is near this value, such as during reversing, the transfer function may approach zero, leading to unpredictable behavior of the output response (Fig.13). In contrast, for forward cruising, the system's dynamics are stable, allowing for easy control of its behavior with a PD controller (Fig.11)

IV. Conclusions

Through linearization, we have developed a PID controller for cruise control and a PD controller for lane changing. Both controllers have been tested under linear dynamics across a range of cruising speeds, yielding satisfactory results that can be applied to real-world situations. Moreover, the cruise controller has been tested with an 8% grade slope disturbance under nonlinear dynamics. Although the performance of the PID controller is somewhat reduced, it still provides adequate results for slope climbing. The lateral PD controller has limitations in its initial response, as the steering angle does not start from zero. Future enhancements to the controller should aim to generate a smooth, sine-like curve for the steering angle. This would ensure that the car operates within its performance limits.

References

[1] Automobile-Catalog, "Car Specs Mercedes-Benz AMG GT Black Series (730 hp) 2021-2022", [Online]. Available: https://www.automobile-catalog.com/car/2021/2968985/mercedes-amg_gt_black_series.html#gsc.tab=0. [Accessed: March 13, 2023]

[2] Polyphony Digital. (2022). Gran Turismo 7 [Software]. Sony Interactive Entertainment.

[3] Vimeo. "New York City Timelapse," Vimeo video, 4:16, 2015. [Online]. Available: https://vimeo.com/manage/videos/812721487.

[4] MathWorks, "MATLAB and Simulink," version 2022b, Natick, MA, USA, 2022.

[5] "Vimeo User Profile: user96991965," Vimeo. Available: https://vimeo.com/user96991965. Accessed: 02 April 2023.

V. Appendix

A. Theoretical Calculation of Rise and Settling Times

The system is linearized at point (2) (120 kph):

$$\dot{v} = -\frac{36.33}{1590}v + \frac{1}{1590}u + \frac{605.5}{1590} \tag{35}$$

Input u is governed by a PID controller:

$$u = K_p(r - v) + K_i\int_0^t (r - v)d\tau + K_d(\dot{r} - \dot{v}) \tag{36}$$

$$\dot{u} = -K_p\dot{v} + K_i(r - v) - K_d\ddot{v} \tag{37}$$

After taking time derivative, eq. (35) becomes:

$$\ddot{v} = -\frac{36.33}{1590}\dot{v} + \frac{1}{1590}\dot{u} \tag{38}$$

$$\ddot{v} = -\frac{36.33}{1590}\dot{v} - \frac{K_p}{1590}\dot{v} + \frac{K_i}{1590}r - \frac{K_i}{1590}v - \frac{K_d}{1590}\ddot{v}$$

$$(1 + \frac{K_d}{1590})\ddot{v} + (\frac{36.33}{1590} + \frac{K_p}{1590})\dot{v} + \frac{K_i}{1590}v = \frac{K_i}{1590}r$$

Rearranging, we have:

$$\ddot{v} + (\frac{K_p + 36.33}{K_d + 1590})\dot{v} + (\frac{K_i}{K_d + 1590})v = (\frac{K_i}{K_d + 1590})r(t) \tag{39}$$

where $r(t)$ is a step input, $r(t) = r \cdot \mathbf{1}(t)$

eq. (39) is of the form (2nd-order linear):

$$\ddot{v} + a\dot{v} + bv = c \cdot \mathbf{1}(t) \tag{40}$$

$$a = \frac{K_p + 36.33}{K_d + 1590} \tag{41}$$

$$b = \frac{K_i}{K_d + 1590} \tag{42}$$

$$c = \frac{K_i}{K_d + 1590}r \tag{43}$$

which can be rewritten in terms of natural frequency and damping ratio, for $t > 0$:

$$\ddot{v} + 2\zeta\omega_n\dot{x} + \omega_n^2 x = c \tag{44}$$

For K_p = 230, K_i = 3.3, K_d = 300, we can calculate the natural frequency and the damping ratio:

$$\omega_n = \sqrt{b} = \sqrt{\frac{K_i}{K_d + 1590}} \tag{45}$$

$$= 0.04179\,\text{rad/s}$$

$$\zeta = \frac{a}{2\omega_n} = \frac{K_p + 36.33}{2\sqrt{K_i(K_d + 1590)}} \tag{46}$$

$$= 1.686$$

The system is overdamped ($\zeta > 1$). Its rise time and settling time cannot be easily obtained analytically. If we were to apply the formulas for underdamped and critically damped systems to obtain a very rough estimate, the rise time and settling time would be:

$$t_r \approx \frac{1.8}{\omega_n} \tag{47}$$

$$= 1.8\sqrt{\frac{K_d + 1590}{K_i}} \tag{48}$$

$$= 43\ s \tag{49}$$

$$t_s = \frac{3.93}{\sigma} \tag{50}$$

$$\approx 8 \cdot \frac{K_d + 1590}{K_p + 36.33} \tag{51}$$

$$= 56.77\ s \tag{52}$$

which is significantly different from $t \approx 15$ s and $t_s \approx 29$ s obtained from simulation.